Quantitative Structure−Property Relationship in a Combinatorial $Bi_{4-x}La_xTi_3O_{12}$ ($0 \leq x \leq 1$) Thin Film Array Obtained with Microbeam XRD and Raman Spectroscopy

Ki Woong Kim, Min Ku Jeon, Tai Suk Kim, Kwang Seok Oh, Joong-Won Shin, and Seong Ihl Woo*

Department of Chemical and Biomolecular Engineering (BK21 Graduate Program) and Center for Ultramicrochemical Process Systems (CUPS), Korea Advanced Institute of Science and Technology (KAIST), 373-1 Guseong-dong, Yuseong-gu, Daejeon 305-701, Republic of Korea

Received March 6, 2007

A ferroelectric $Bi_{4-x}La_xTi_3O_{12}$ (BLT) thin film library was fabricated from $Bi_2O_3/La_2O_3/TiO_2$ multilayers using a multitarget RF-sputtering system equipped with an automated shutter. The polarization−electric field and structure were mapped as a function of the La content from $x = 0$ to 1. Remnant polarization (P_r) increased as the La content decreased, and it reached a maximum $2P_r$ of 20 $\mu C/cm^2$ at $x = 0.28$. At $x < 0.28$, $2P_r$ decreased gradually as the La content decreased. This compositional dependence of the remanent polarization was the result of the degree of TiO_6 tilting along the $a-b$ plane changing as a function of the La content. This was quantitatively related to the intensity ratio between the (117) peak and the (008) peak in the X-ray diffraction (XRD) pattern and to the intensity of the Raman band at 848 cm^{-1}, arising from stretching mode of TiO_6 octahedrons.

Introduction

Bismuth-layered perovskite ferroelectric films, including $SrBi_2Ta_2O_9$ (SBT)[1] and $(Bi,La)_4Ti_3O_{12}$ (BLT),[2] have drawn interest as ferroelectric random-access memory (FRAM) because of their fatigue-free properties over 10^{10} read/write cycles when used with a Pt electrode in contrast to those of $Pb(Zr,Ti)O_3$ (PZT).[3] However, these materials have the disadvantage of having a smaller remanent polarization (P_r) compared to that of PZT. To improve the remnant polarization (P_r), numerous attempts have been made to substitute lanthanide group atoms for the Bi site in $Bi_4Ti_3O_{12}$ (BTO), and it was demonstrated that the P_r value is strongly dependent on the chemical composition related to bismuth volatility.[4] However, so far, most studies have focused on the optimization of the deposition process variables in fabricating ferroelectric material with a specific chemical composition such as $Bi_{3.25}La_{0.75}Ti_3O_{12}$.[5]

To verify the compositional dependence of P_r in a ferroelectric material, a combinatorial approach is very efficient because it is possible to fabricate a large number of thin film library samples with various chemical compositions on a wafer under the same deposition conditions.[6] Therefore, in our contribution, a combinatorial methodology was applied to the fabrication of a $Bi_{4-x}La_xTi_3O_{12}$ (BLT, $0 \leq x \leq 1$) thin film library to optimize the chemical composition for large P_r and to find quantitative structure−property relationships (QSPR) in BLT libraries.

Experimental Section

Multitarget Sputtering System. This equipment was designed to fabricate a thin film library by means of the pulsed laser-deposition (PLD) method with an automated shutter.

* To whom correspondence should be addressed. E-mail: siwoo@kaist.ac.kr. Phone: +82-42-869-3918. Fax: +82-42-869-8890.

As shown in Figure 1, there are four target guns, and positions of the targets can be changed by a rotation mechanism. The automated shutter produces the concentration gradient over the substrate along the *x*-axis. All deposition procedures are operated by the software program. In the design of the equipment, we considered the following two criteria: (1) thickness uniformity and (2) thermal uniformity. In RF-sputtering, it is especially difficult to produce a uniform thickness because the plasma was generated in a spiral type, and therefore, the center was thicker than the edges. To overcome these problems, we deposited the thin film library in a restricted region (4×4 cm^2) by using a target with a 4 in. diameter. This thickness deviation was ±1% at 250 nm, and the thermal uniformity was less than 3% at 500 °C on wafer with a diameter of 4 in.

High-Throughput Synthesis of $Bi_{4-x}La_xTi_3O_{12}$ (BLT) Thin Film Array. We used a multitarget RF-sputtering (Sunicoat-524, manufactured by Sunic Inc., Korea) system equipped with an automated shutter. To fabricate the ferroelectric BLT thin film library, Bi_2O_3, TiO_2, and La_2O_3 (purity = 99.999%, diameter = 4 in.) were used as targets. Before fabricating the thin film library, we measured the deposition rate of each target material as shown in Table 1.

Initially, TiO_2 was deposited on the (111) $Pt/TiO_2/SiO_2/Si$ substrate (4×4 cm^2) for 145 s without moving the shutter (RF power = 300 W, Ar/O_2 = 15/5 sccm). After the deposition, we changed the target material from TiO_2 to Bi_2O_3, and deposited this material for 17 s without moving the shutter (RF power = 50 W, Ar/O2 = 15/5sccm). To give the Bi/La concentration gradient along the *x*-axis, Bi_2O_3 was deposited with moving the shutter forward, and then La_2O_3 was deposited with moving the shutter backward. Here, the

10.1021/cc0700400 CCC: $37.00
Published on Web 08/01/2007

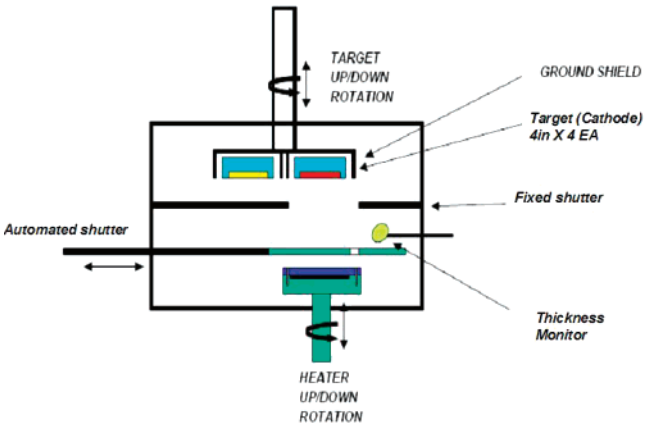

Figure 1. Schematic drawing of multitarget sputtering system with automated shutter.

Table 1. Deposition Rate of Target Materials Using the RF-Sputtering System

target material	RF power (W)	Ar/O_2 (sccm)	deposition rate (nm/min)
Bi_2O_3	50	15/5	12.8 ± 0.05
La_2O_3	100	15/5	1.87 ± 0.05
TiO_2	300	15/5	1.11 ± 0.05

speeds of the movable shutter for Bi_2O_3 and La_2O_3 were 0.35 and 0.06 cm/s, respectively, according to the deposition rate.

The motion of the shutter was synchronized with the plasma generation in such a way that for each deposition, a thickness gradient was created on the substrate. Finally, Bi_2O_3 and TiO_2 were deposited sequentially, as previously described. Thus, a sandwich structure of $TiO_2/Bi_2O_3/Bi_2O_3/La_2O_3/Bi_2O_3/TiO_2$ with a thickness of 15.4 nm was fabricated as shown Figure 2. The chemical composition was measured by wavelength dispersive spectroscopy (WDS). The compositional error range was within 0.1%.

This process is called a 1-deposition cycle. To obtain a film (BLT thin film library) with the thickness of 250 nm, we performed 16 deposition cycles. During the deposition, the substrate temperature was maintained at 300 °C for efficient intermixing of each material and to prevent the Ti ion from migrating onto the Pt surface.[7] A gas mixture of Ar and O_2 (Ar/O_2 = 3:1, total flow rate = 20 sccm) was used to suppress the formation of oxygen vacancies. The process pressure was 5×10^{-3} Torr, and the base pressure was approximately 5×10^{-6} Torr. After the deposition, the BLT thin film library was heat treated at 400 °C for 1 h under O_2 and postannealed at 700 °C for 5 h under an oxygen atmosphere for the crystallization.

Characterization of the $Bi_{4-x}La_xTi_3O_{12}$ (BLT) Thin Film Array. To analyze the new crystallographic phase and the preferred orientation of as-prepared thin film library, we used microbeam XRD (D8 DISCOVER with GADDS for combinatorial screening by Bruker-AXS) with a small beam size (<500 μm), and the *xyz* manipulator was controlled by a computer software. The angle between the detector and the substrate was 20°, and that between the X-ray gun and the substrate was 15°. The XRD mapping was performed in $\theta-2\theta$ scan type with Cu Kα radiation (λ = 1.5405 Å) and was operated at 40 mA and 40 kV. A Micro-Raman system (manufactured by Dong Woo Optron Ltd. & Photon Design Co.) was used to map the local structure including various metal−oxygen vibration modes as a function of La content. When the Raman spectra were obtained, the Ar laser (λ = 488 nm, Power = 40 mW) was incident on the sample, and the detection time was 10 s per sample. To improve the signal-to-noise ratio, we used a holographic-type monochromator and a back-illuminated photoarray detector with high-sensitivity (liquid nitrogen cooled, 1340 × 400 pixels, manufactured by Princeton Co.). Therefore, we were able to obtain good-quality Raman spectra in a relatively short time (less than 10 s) without compromising the signal-to-noise ratio. The chemical composition of the prepared combinatorial array was obtained by wavelength dispersive spectroscopy (WDS, Microspec 3-PC). The surface morphology and cross-sectional image of thin film library were analyzed by scanning electron microscope (SEM, Philips 533M) for a measurement of film thickness. To measure the electrical properties, Pt electrodes with a 200-μm diameter were deposited on the thin film library using the RF-magnetron sputtering system. The ferroelectric properties, including $P-E$ hysteresis, were measured using a Radiant Technology RT66A ferroelectric tester at 10 V.

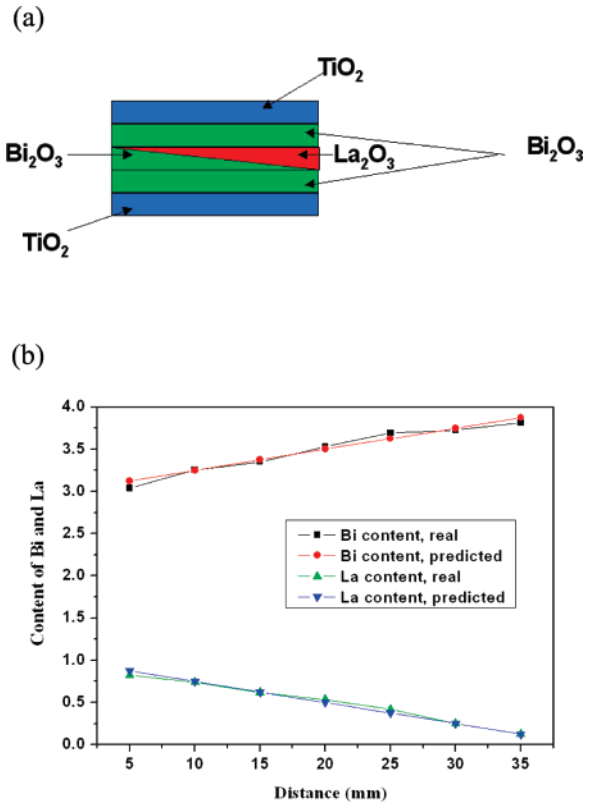

Figure 2. (a) Schematic diagram of a $Bi_{4-x}La_xTi_3O_{12}$ thin film library generated from $TiO_2/Bi_2O_3/La_2O_3/TiO_2$ multilayers using the multitarget sputtering system. (b) The chemical composition of $Bi_{4-x}La_xTi_3O_{12}$ in the *x* direction. This was measured by WDS, and the compositional error is ±0.1%.

Results and Discussion

To analyze the polarization−electric field ($P-E$) characteristics of the BLT thin film library as a function of the La content (x), we deposited a Pt top electrode (diameter = 200 μm) on the BLT thin film library to form a capacitor structure. As shown in Figure 3, the remanent polarization

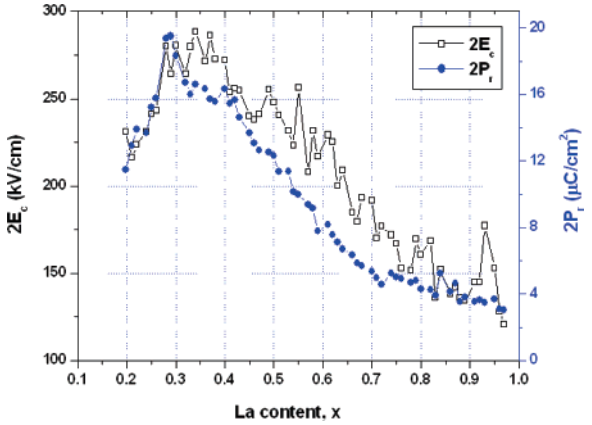

Figure 3. Remnant polarization and coercive field of $Bi_{4-x}La_xTi_3O_{12}$ as a function of La content, *x*.

increased as the La content (*x*) decreased, and it reached the largest value of 20 μC/cm^2 at $x = 0.28$. However, in the region of $x < 0.28$, P_r decreased gradually as the La content decreased. In particular, at $x < 0.2$, the $P-E$ hysteresis loop could not be measured because of oxygen vacancies accompanied by Bi defects. The oxygen vacancies accumulate in the electrode (Pt)−ferroelectric capacitor (BLT) interface and cause domain pinning which leads to smaller P_r and higher leakage of current density.[8] Therefore, the $P-E$ characteristic of the BLT thin film library showed that a small amount of La substituted for Bi ($x < 0.2$) did not effectively reduce the defect concentration arising from Bi volatility.

It is important to improve the remnant polarization because it acts as the sensing margin to discriminate "0" and "1" in a binary memory code. Simultaneously, a low coercive field (E_c) is necessary to lower the operating voltage in FRAM. As shown in Figure 3, the change in coercive field is proportional to that in P_r because coercive field is the electric field required to reduce polarization to zero. The $2E_c$ value was about 260−280 kV/cm at $0.26 < x < 0.32$, and this value is relatively greater than that of PZT. This is caused by the $Bi_4Ti_3O_{12}$ structure having a *c*-axis parameter (about 3.2 nm) that is longer than that of PZT (about 0.5 nm). In such a structural system, more energy is needed to switch the aligned dipole direction than in PZT.

The thin film library was analyzed with microbeam X-ray diffraction in the $18° \leq 2\theta \leq 52°$ range to confirm the crystallographic phase and preferred orientation. As shown in Figure 4a, the samples on the library had no impurity phases (i.e., $Bi_2Ti_2O_7$) and binary oxide including Bi_2O_3, TiO_2 and La_2O_3 in the compositional range of *x* between 0 and 1. In the X-ray diffraction (XRD) patterns, the crystalline growth in the (117) direction increased as the La content decreased to 0.2. At $x = 0.2$, a slight increase in the (00*n*) diffraction peak was observed, and at $x \leq 0.1$, a remarkable amount of growth in *c*-axis direction was observed instead of an abrupt decrease in the peak intensity in the (117) direction. In $Bi_4Ti_3O_{12}$, the spontaneous polarization (P_s) was negligible along the *c*-axis because the vector of the P_s in bismuth-layered perovskite materials lies along the *a*-axis.[9] This allowed us to choose the structural parameter, R117, to consider such an anisotropic property. R117 denotes the peak intensity ratio between the (117) diffraction peak and

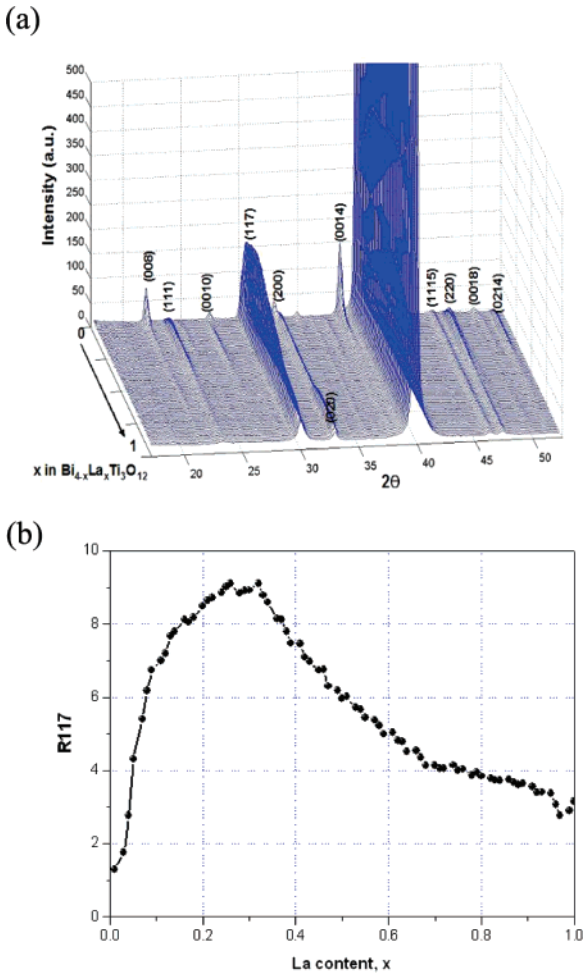

Figure 4. (a) Microbeam X-ray diffractogram of $Bi_{4-x}La_xTi_3O_{12}$ as a function of La content, *x* ($0 < x < 1$). (b) The intensity ratio between the (117) and (008) peaks plotted as a function of La content, *x*.

the (008) diffraction peak. This value was the maximum in the region of the La content (*x*) between 0.26 and 0.32. (Figure 4b). This trend is similar to the correlation of chemical composition with P_r, as shown in Figure 3. This is a valuable design criterion to develop high-P_r perovskite-type ferroelectric oxides. At high *x*, intensity of XRD peaks decreased significantly, indicating the low crystallinity of BLT at this region.

The polarization of BLT originates from distortion of TiO_6 octahedrons. BLT has a monoclinic structure and loses its ferroelectricity when the crystal structure changes to a tetragonal structure. As shown in a previous report,[10] TiO_6 octahedrons are present as a distorted form in the monoclinic BLT, and the degree of distortion of the TiO_6 octahedrons determines magnitude of polarization. We analyzed the distortion of the TiO_6 octahedrons for a further quantitative structure−property relationship (QSPR) study of the BLT library and a micro-Raman spectroscopic approach was carried out for the analysis of structural changes in TiO_6 octahedrons because it can provide information on Ti−O bonding vibrations with a short measurement time.

Figure 5a displays Raman shifts of the BLT film. Three intense peaks were observed at 260, 550, and 848 cm^{-1} when $x = 0$ and were assigned to the internal angle bending

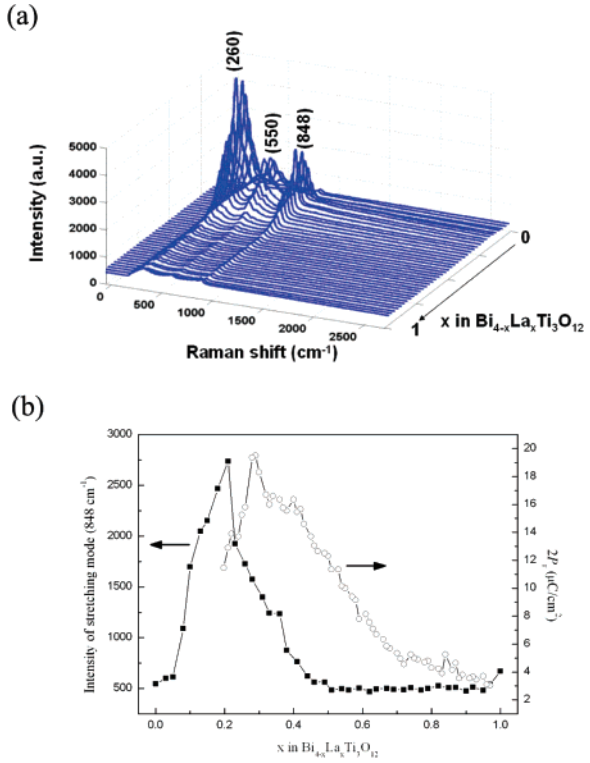

Figure 5. (a) Micro-Raman spectra of $Bi_{4-x}La_xTi_3O_{12}$ as a function of La content, x. (b) The intensity of the Raman-active peak at 848 cm^{-1} as a function of La content. The Ar laser ($\lambda = 488$ nm, $P =$ 40mW) was incident on the sample, and the detection time was 30 s per sample.

vibration, combination of stretching and bending vibrations, and another stretching vibration, respectively.[11] Figure 5b shows the intensity of the Ti−O stretching vibration mode at 848 cm^{-1} and $2P_r$ as a function of the La content. This peak intensity started to increase at $x = 0.4$ with decreasing La content and reached a maximum at $x = 0.21$. At $x < 0.2$, there was an abrupt decrease in the intensity of the peak corresponding to the stretching mode. Considering that $\mu = \alpha E$, where μ is the induced dipole moment, α is the polarizability, and E is the electric field of the incoming radiation, the strong intensity of the Raman peak implies large polarization because the the Raman peak intensity is $I \propto (\int \psi_{v'}^* \alpha \psi_{v''} d\tau)$,[2] where $\psi_{v'}$ and $\psi_{v''}$ are wave functions of the upper and lower vibrational quantum states, respectively, and $d\tau = dxdydz$, where x, y, and z are the nuclear coordinates in the molecular frame.[12] The weakening of the 848 cm^{-1} band indicates that near absence of the La atoms in BLT resulted in a highly ordered crystal structure. Since the polarization of TiO_6 octahedrons dominates the total P_r of BLT, the intensity of the peak at 848 cm^{-1} is a good indicator for a rapid and precise measurement of polarization of BLT. Here, we found that the maximum content of La from the $P-E$ hysteresis (maximum at $x = 0.28$) was different from that of the micro-Raman spectroscopic (maximum at $x = 0.21$) analysis. This difference results from the interface properties between BLT and Pt electrodes, whereas the spectroscopic approach is not affected by the Pt top and bottom electrodes. The Pt electrodes are essential for measurement of polarization, and problems such as charge accumulation and domain pinning can occur in BLT−Pt interfaces.[8] These phenomena reduce the measured $2P_r$, and therefore, smaller $2P_r$ values can be obtained despite intense Raman peaks. Although this interface problem of BLT caused a mismatch of the optimum composition between the $P-E$ hysteresis and the Raman spectroscopic results, the micro-Raman spectroscopy is still a useful method in the QSPR study of combinatorial libraries because it provides reliable structural information within a short measurement time.

In conclusion, a $Bi_{4-x}La_xTi_3O_{12}$ thin film library ($0 \leq x \leq 1$) was fabricated from $Bi_2O_3/La_2O_3/TiO_2$ multilayers using RF-multitarget sputtering. The linear compositional gradient over the substrate was obtained using an automated shutter. In a $P-E$ hysteresis loop, $Bi_{3.72}La_{0.28}Ti_3O_{12}$ exhibited the greatest $2P_r$ value, 20 $\mu C/cm^2$. For $x < 0.2$, the $P-E$ hysteresis loop could not be measured because of the higher leakage of current density. Microbeam XRD and a micro-Raman systems were used for the QSPR study. The intensity ratio between the (117) and (008) peaks of XRD spectra and intensity of the 848 cm^{-1} peak exhibited that the $2P_r$ values are in agreement, which implies that these two parameters are good indicators for QSPR analysis.

Acknowledgment. This research was funded by the Center for Ultramicrochemical Process Systems (CUPS) sponsored by KOSEF (2007).

References and Notes

(1) Scott, J. F.; Ross, F. M.; Paz de Araujo, C. A.; Scott, M. C.; Huffman, M. *MRS Bull.* **1996**, *21*, 33.
(2) Park, B. H.; Kang, B. S.; Bu, S. D.; Noh, T. W.; Lee, J.; Jo, W. *Nature* **1999**, *401*, 682−685.
(3) (a) Scott, J. F.; Araujo, C. A. *Science* **1989**, *246*, 1400−1405. (b) Sreenivas, K.; Sayer, M. *J. Appl. Phys.* **1988**, *64*, 1484−1493. (c) Li, Y.; Nagarajan, V.; Aggarwal, S.; Ramesh, R.; S-Riba, L. G.; M-Miranda, L. J. *J. Appl. Phys.* **2002**, *92*, 6762−6767.
(4) (a) Uchida, H.; Yoshikawa, H.; Okada, I.; Matsuda, H.; Iijima, T.; Watanabe, T.; Kojima, T.; Funakubo, H. *Appl. Phys. Lett.* **2002**, *81*, 2229−2231. (b) Chon, U.; Kim, K. B.; Jang, H. M.; Yi, G. C. *Appl. Phys. Lett.* **2001**, *79*, 3137−3139. (c) Watanabe, T.; Funakubo, H.; Osada, M.; Noguchi, Y.; Miyayama, M. *Appl. Phys. Lett.* **2002**, *80*, 100−102. (d) Jeon, M. K.; Chung, H. J.; Kim, K. W.; Oh, K. S.; Woo, S. I. *Thin Solid Films* **2005**, *489*, 1−4.
(5) (a) Wu, D.; Li, A.; Zhu, T.; Liu, Z.; Ming, N. *J. Appl. Phys.* **2000**, *88*, 5941−5945. (b) Chon, U.; Yi, G.-C.; Jang, H. M. *Appl. Phys. Lett.* **2001**, *78*, 658−660. (c) Choi, T.; Kim, Y. S.; Yang, C. W.; Lee, J. *Appl. Phys. Lett.* **2001**, *79*, 1516−1518. (d) Zhai, J.; Chen, H. *Appl. Phys. Lett.* **2003**, *20*, 442−444.
(6) (a) Xiang, X. D.; Sun, A.; Briceno, G.; Lou, Y.; Wang, K. A.; Chang, H.; W-Freedman, W. G.; Chen, S. W.; Schultz, P. G. *Science* **1995**, *268*, 1738−1740. (b) Wang, J.; Yoo, Y. K.; Gao, C.; Takeuchi, I.; Sun, X. D.; Chang, H.; Xiang, X.-D.; Schultz, P. G. *Science* **1998**, *279*, 1712−1714. (c) Takeuchi, I.; Chang, H.; Gao, C.; Schultz, P. G.; Xiang, X.-D.; Sharma, R. P.; Downes, M. J.; Venkatesan, T. *Appl. Phys. Lett.* **1998**, *73*, 894−896. (d) Reddington, E.; Sapienze, A.; Gurau, B.; Viswanathan, R.; Sarangapani, S.; Smotkin, E. S.; Mallouk, T. E. *Science* **1998**, *280*, 1735−1737. (e) Jandeleit, B.; Schaefer, D. J.; Powers, T. S.; Turner, H. W.; Weinberg, W. H. *Angew. Chem., Int. Ed.* **1999**, *38*, 2494−2532. (f) Yoo, Y. K.; Xiang, X. D. *J. Phys.: Condens. Matt.* **2002**, *14*, R49−R78. (g) Smith, R. C.; Hoilen, N.; Roberts, J.; Campbell, S. A.; Gladfelder, W. L. *Chem. Mater.* **2002**,

14, 474−476. (h) Amis, E. J. *Nat. Mater.* **2004**, *3*, 83−85. (i) Koinuma, H.; Takeuchi, I. *Nat. Mater.* **2004**, *3*, 429−438. (j) Woo, S. I.; Kim, K. W.; Cho, H. Y.; Oh, K. S.; Jeon, M. K.; Kim, T. S.; Tarte, N. H.; Mahmood, A. *QSAR Comb. Sci.* **2005**, *24*, 138−154. (k) Kim, K. W.; Jeon, M. K.; Oh, K. S.; Kim, T. S.; Kim, Y. S.; Woo, S. I. *Proc. Natl. Acad. Sci. U.S.A.* **2007**, *104*, 1134−1139.

(7) Nagata, H.; Chikushi, N.; Takenaka, T. *Jpn. J. Appl. Phys.* **1999**, *38*, 5497−5499.

(8) Noguchi, Y.; Miyayama, M. *Appl. Phys. Lett.* **2001**, *78*, 1903−1905.

(9) (a) Cummins, S. E.; Cross, L. E. *J. Appl. Phys.* **1968**, *39*, 2268−2274. (b) Lee, H. N.; Hesse, D.; Zakharov, N.; Gosele, U. *Science* **2002**, *296*, 2006−2009.

(10) (a) Shimakawa, Y.; Kubo, Y.; Tauchi, Y.; Asano, H.; Kamiyama, T.; Izumi, F.; Hiroi, Z. *Appl. Phys. Lett.* **2001**, *79*, 2791−2793. (b) Jeon, M. K.; Kim, Y.-I.; Sohn, J. M.; Woo, S. I. *J. Phys. D: Appl. Phys.* **2004**, *37*, 2588−2592. (c) Jeon, M. K.; Kim, Y.-I.; Nahm, S.-H.; Woo, S. I. *J. Phys. Chem. B* **2005**, *109*, 968−972. (d) Jeon, M. K.; Kim, Y.-I.; Nahm, S.-H.; Woo, S. I. *J. Phys. D: Appl. Phys.* **2006**, *39*, 5080−5085.

(11) Kojima, S.; Imaizumi, R.; Hamazaki, S.; Takashige, M. *Jpn. J. Appl. Phys.* **1994**, *33*, 5559−5564.

(12) Bernath, P. F. *Spectra of Atoms and Molecules*; Oxford University Press: New York, 1995; pp 283−296.

CC0700400